Characterization of precipitates in a 7.9Cr–1.65Mo–1.25Si–1.2V steel during tempering

*H. Djebaili**, *H. Zedira*, *A. Djelloul*, *A. Boumaza*

LASPI^2*A Laboratoire des Structures, Propriétés et Interactions Inter Atomiques, Centre Universitaire Khenchela, Algeria*

ARTICLE DATA

Article history:
Received 7 January 2009
Accepted 11 March 2009

Keywords:
Tempering
Hot hardness
Carbides
Secondary hardening
Precipitates

ABSTRACT

In this paper, the precipitates formed during the tempering after quenching from temperature 1150 °C for 7.90Cr–1.65Mo–1.25Si–1.2V steels are investigated using an analytical transmission electron microscope (A-TEM).The study of this tempering is carried out in isothermal and anisothermal conditions, by comparing the results given by dilatometry and hot hardness. Tempering is performed in the range of 300–700 °C. Coarse primary carbides retained after heat treatment are V-rich MC and Cr–Mo-rich M_7C_3 types. In turn, it gives a significant influence on the precipitation of fine secondary carbides, that is, secondary hardening during tempering. The major secondary carbides are Cr–Mo–V-rich M′C (and/or) Cr–Mo-rich M_2C type. The peak hardness is observed in the tempering range of 450–500 °C. In the end, we observe between 600 and 700 °C, that this impoverished changes the phase. At these high temperatures of tempering, we observe that there is a carbide formation of the types M_6C developing at the expense of the fine M_7C_3 carbides previously formed.

1. Introduction

The purpose of the present work is to study new nuances of steels likely to be used to manufacture hot rolls. The choice was made on chromium–molybdenum–silicon steels, intended to replace other materials, such as cast iron with high chromium content. From the above mentioned elements of addition, these alloys have a specific addition of vanadium, to modify the nature as well as the morphology of primary carbides and to confer a secondary hardening by precipitation of fine carbides [1] of the type M′C (V_4C_3).

The nuance studied here results from modifications of composition made to a more traditional alloy containing Cr (12%), but less Mo (1.5%). These modifications have been done, on one hand to decrease the volumic fraction of primary carbides being able to be at the origin of the crack initiation in service. On the other hand, they allow the formation of oxidized surface layers low thickness exerting a protective action with respect to later oxidation (such oxide coatings have not a notable role on the starting of fissures). The reduction in the chromium content is partially compensated by an increase in the molybdenum amount. We observe that the hot resistance of the matrix is caused by the increasing of this element.

2. Experimental Procedure

Cr–Mo–Si–V steel samples of 5 mm×5 mm×20 mm size, having specified chemical composition (C: 0.80%, Cr: 7.90%, Mo: 1.65%, Si: 1.25%, V: 1.2%, balance Fe) are heated at 1050 and 1150 °C during 15 mn, followed by a water quenching.

After the last quenching (50 °C/s) from θ_γ>1050 °C, the structure consists of martensite (α'), residual austenite (volumic fraction of this phase — determined by the integrated intensities method [2,3] — is retained at 20 °C: up to 20% for θ_γ>1150 °C) and non-dissolved primary carbides of the types M_7C_3 and MC [4–9].

In the quenched state, the material has a high hardness and a low capacity of deformation, thus it is advisable to temper it to

* *Corresponding author*. Tel.: +213 32331960.
E-mail address: h_djebaili@yahoo.fr (H. Djebaili).

1044-5803/$ – see front matter © 2009 Elsevier Inc. All rights reserved.
doi:10.1016/j.matchar.2009.03.007

confer more appropriate mechanical characteristics. In addition, a very fine carbide precipitation, more or less coherent with the matrix, can intervene and contribute to maintain the hardness of the steel at a high level (secondary hardening).

The effect exerted by the initial composition of the γ matrix on the structural evolutions developed during tempering will be analyzed mainly in two ways:

- Initially, by metallographic examination after isochronous and/or isothermal thermal treatments and by hardness testing,
- Then, in anisothermal condition, by complementary tests by dilatometry, thermo-magnetometry and differential thermal analysis.

These tests were performed with a heating rate got to 300 °C/h under primary vacuum (5×10^{-2} Torr, i.e. 6.65 Pa).

3. Results and Discussion

3.1. *Anisothermal Tempering*

Fig. 1 shows two differential dilatometric curves corresponding to samples respectively tempered after previously water quenching from austenitization θ_γ temperatures. Anomalies are observed in different intervals of temperature between 20 °C and the Ac1 temperature. We observe initially two successive contractions: stage I and II developing between 50 and 350 °C. From 350 to 500 °C, the curve is appreciably linear. It must be noted that after quenching from 1150 °C, the slope of the curve is more significant: this is due to the presence of a significant quantity of residual austenite in the initial state.

A first expansion is observed between 500 and 600 °C (stage III), which is especially marked if θ_γ=1150 °C. Then, a second one is developing between 600 and 700 °C (stage IV).

As from 700 °C and up to the point Ac1, a contraction occurs (stage V).

In order to specify some of the phenomena observed, non-cumulative tempering were performed up to various

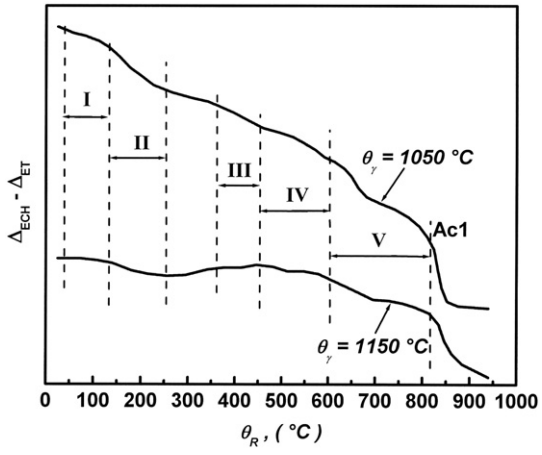

Fig. 1 – Dilatometric curves recorded on heating from different quenched states (from 1050 and 1150 °C).

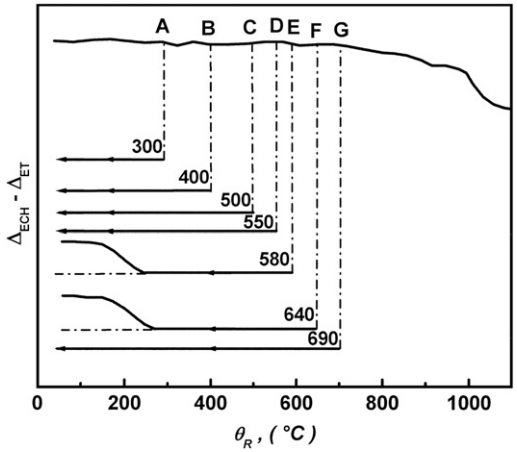

Fig. 2 – Dilatometric curves recorded on cooling after non isothermal tempering up to different θ_R temperatures.

temperatures θ_R, the curves recorded on cooling show that (Fig. 2):

- If θ_γ=1050 °C, no anomaly is observed during these cooling where $300<\theta_R<700$ °C,
- If θ_γ=1150 °C, no anomaly is observed on cooling for $300<\theta_R<550$ °C, while for $\theta_R>550$ °C (for example θ_R=580 or 640 °C), an expansion occurs on cooling at a temperature:
- Relatively low (300 °C) if θ_R=580 °C,
- Slightly higher (350 °C) if θ_R=640 °C.

3.2. *Thermomagnetometry*

Fig. 3 gathers curves recorded by thermomagnetometry, that schematizes the variations of *J* (intensity of magnetization) observed. From this, we can conclude that:

- between 100 and 350 °C, there is a first increase in *J* (stages I′ and II′),
- a weak or no evolution intervenes between 350 and 480 °C,

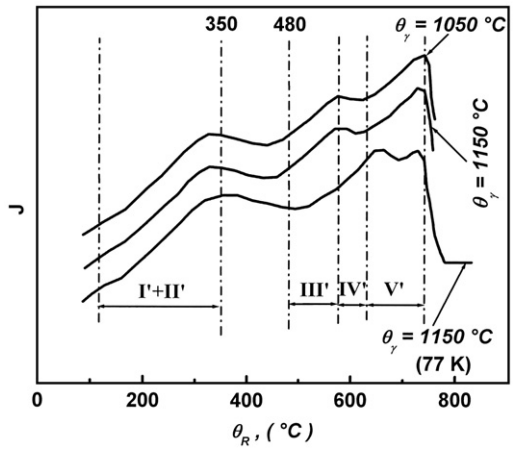

Fig. 3 – Thermomagnetic curves recorded on heating from samples heated at austenizing temperatures (1050 and 1150 °C) then water quenched. For θ_γ=1150 °C, a sample was first quenched down to 20 °C then to 77 K before tempering.

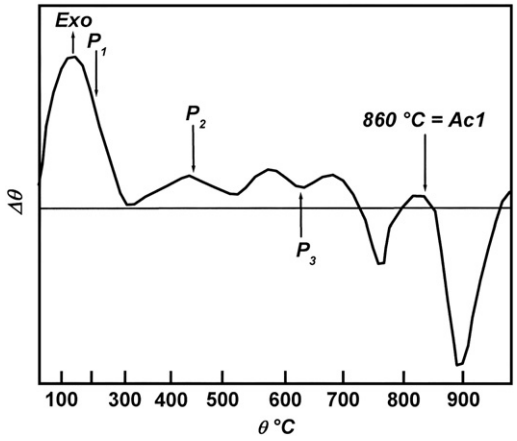

Fig. 4 – Differential thermal analysis curve from a sample quenched from 1150 ° C.

– between 480 and 600 °C, a second increase in *J* develops (stage III′),
– between 600 and 650 °C, a weak reduction in *J* (stage IV′) happens,
– finally, a third increase in *J* is observed from 650 °C up to Curie point θ_c=1150 °C (stage V′).

3.3. *Differential Thermal Analysis*

The behavior during tempering of a sample quenched from 1150 °C was also followed by differential thermal analysis. Fig. 4 represents the curve obtained, it can be noted that:

– between 50 and 275 °C, there is a first exothermic reaction (peak P_1),
– between 275 and 480 °C approximately, a second exothermic reaction with lower amplitude develops (peak P_2).
– A third exothermic peak (P_3) spreads out between 480 and 720 °C approximately. This peak is obviously duplicated; the first component is between 480 and 640 °C, while the second is spread out from 640 to 720 °C.
– The pseudo-endothermic anomaly that observed corresponds to the variation of C_P preceding the crossing of the point of Curie, which is reached at 755 °C.
– The austenitic transformation (endothermic peak) begins at 860 °C.

3.4. *Isothermal Tests*

The various methods of analysis previously used have given much information without however making it possible to visualize and locate carbides formed during different temperings. Consequently, we were brought to carry out examinations on thin foils by transmission electron microscopy. These foils were taken in samples quenched from 1150 °C, then tempered at various temperatures θ_R.

Fig. 5a corresponds to a sample treated 1 h at 415 °C. We easily distinguish the martensite needles in which fine lengthened particles are distributed. The pattern Fig. 5b corresponds to carbides of the type M_3C.

A tempering carried out at a temperature higher than that of the peak of secondary hardening (that is to say 500 °C), causes a notable modification of the structure. Thus, after tempering 1 h at 550 °C, we observe that precipitates having the shape of rods, like a very fine and more abundant precipitation within the matrix (Fig. 6a). The fine precipitates are identified as being of type M′C (Fig. 6b, M′C = variant of MC). On the other hand, carbides having the shape of rods are of the type M_7C_3. Let us notice however that carbides of the type M_2C [10] were not detected during these examinations.

This is due to the fact that these carbides precipitate in a so fine form that an implemented tempering is not sufficient so that they may acquire a size such as diagrams of electronic micro-diffraction might be recorded.

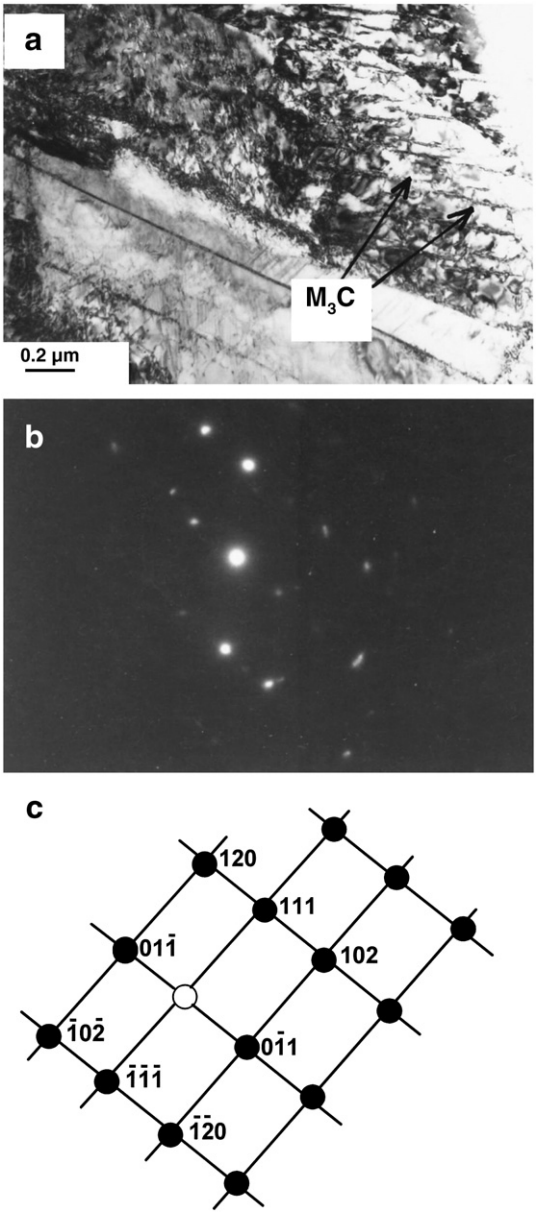

Fig. 5 – a) Bright field observation after tempering at θ_R=415 °C; b) Electron diffraction pattern: [2 1 $\bar{2}$] M_3C. c) Sketch of the selected zone diffraction pattern: [2 1 $\bar{2}$] M_3C.

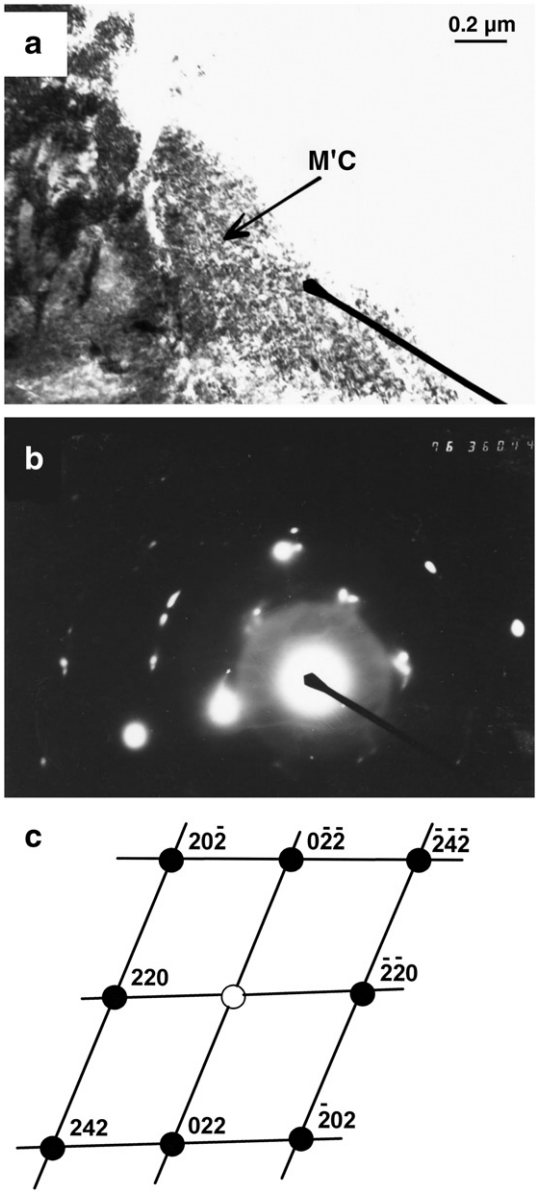

Fig. 6 – a) Bright field observation after tempering at θ_R = 550 °C; b) Electron diffraction pattern: [1 $\bar{1}$ 1] M′C. c) Sketch of the selected zone diffraction pattern: [1 $\bar{1}$ 1] M′C.

In the case of a sample having undergone a 1 h tempering at 625 °C, carbides M_7C_3 are still observed having a lengthened form (Fig. 7a, and b).

If the tempering temperature is increased up to 700 °C (t = 1 h), the preceding carbides disappeared and new carbides are observed:

- Some of them are relatively large and their shape is rather geometrical. These carbides are of the type M_6C and they were identified by micro-diffraction (Fig. 8a, and b).
- Other carbides are localized on the grain boundaries [10,11] of the matrix. They are type $M_{23}C_6$ carbides as the stereotype to micro-diffraction of Fig. 8b testifies. Let us recall that these carbides result probably from the carbides M_7C_3 "in-situ" transformation [12].

3.5. *Discussion*

On the basis of the results observed, five successive stages can be distinguished.

Stage I ($50 < \theta_R < 250$°C)

The martensitic structure (α') is subjected to a distressing accompanied by a fall in hardness. In parallel, this phase impoverishes out of carbon due to the precipitation of ε carbide ($Fe_{2,4}C$) [13–15]. This carbide, with a hexagonal structure, is the first to be formed during a treatment of tempering, it is not thermodynamically stable, but among all

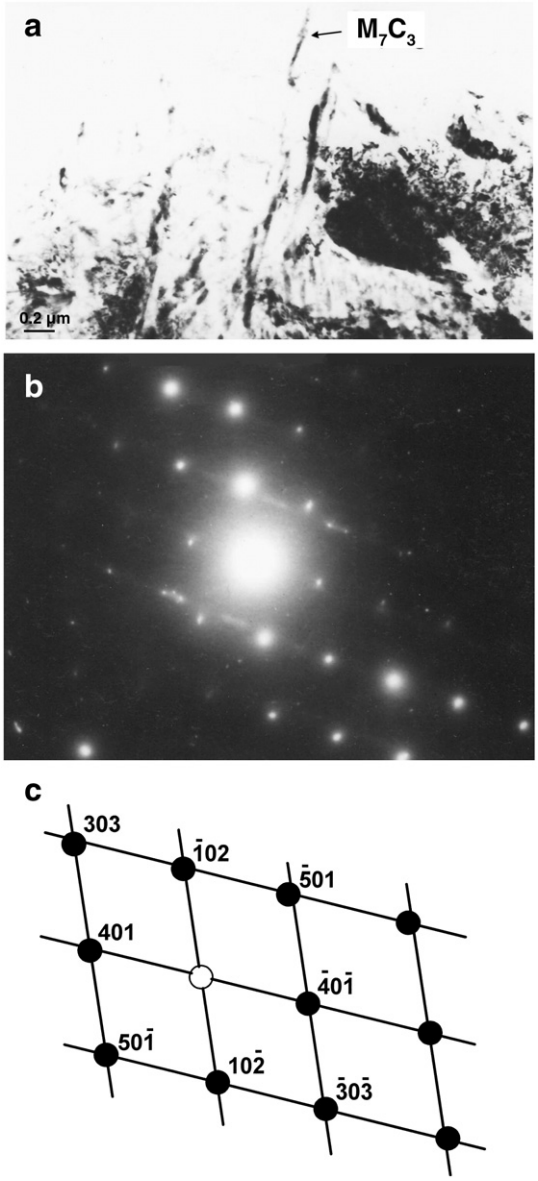

Fig. 7 – a) Bright field observation after tempering at θ_R = 635 °C; b) Electron diffraction pattern: [0 9 0] M_7C_3. c) Sketch of the selected zone diffraction pattern: [0 9 0] M_7C_3.

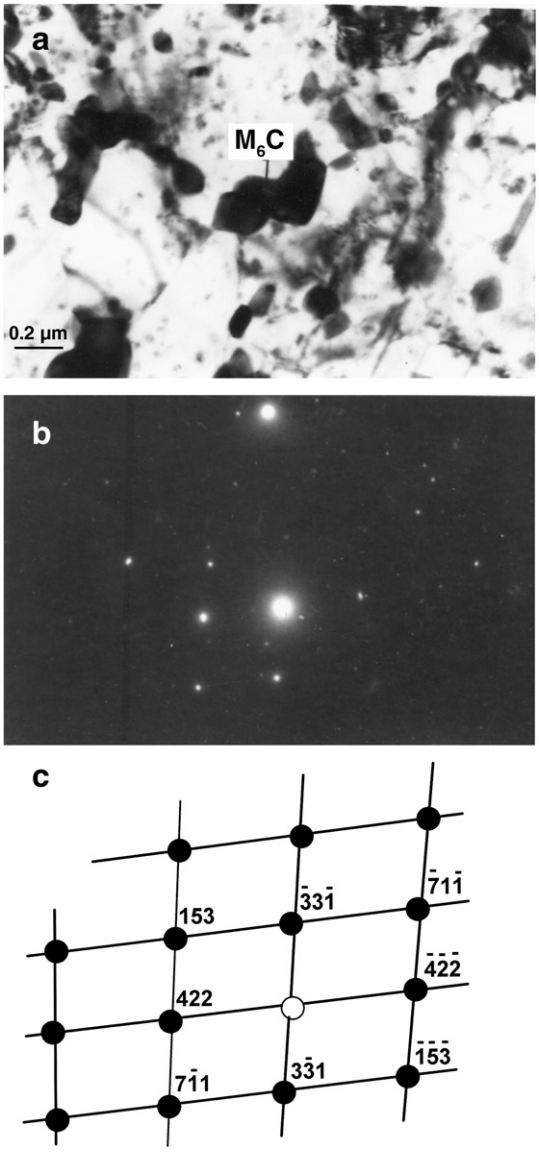

Fig. 8 – a) Bright field observation after tempering at θ_R = 700 °C; b) Electron diffraction pattern: [1 1 $\bar{4}$] M_6C. c) Sketch of the selected zone diffraction pattern: [1 1 $\bar{4}$] M_6C.

of the iron carbides it is the one that generates less accommodation stresses with respect to the matrix. This process is accompanied by a contraction, an increase in *J* and a heat release (peak P_1).

Stage II ($250 < \theta_R < 350$°C)

The martensitic structure, already somewhat impoverished by the precipitation of the ε carbide, continues to reject carbon; in addition, the carbide ε, previously formed, dissolves. The released carbon gives precipitates in the form of substituted cementite M_3C [16]. This evolution results in a second contraction, while *J* continues to increase (the martensitic matrix being enriched in iron). In addition, the exothermic reaction P_1, is completed while a second exothermic reaction P_2 starts. Lastly, the hardness of material tends to be stabilized owing to the fact that the elimination of the internal stresses is completed while the matrix is somewhat hardened by fine formed carbides (containing iron). However, only the carbides of the type M_3C could be identified.

Stage III″ or III: In fact, it is necessary to define two intervals of temperature:

- $350 < \theta_R < 480$–500 °C: Hardness increases clearly for finally reaching a maximum (Fig. 9, curve .1), but the sample expansion or the thermo-magnetometric behavior do not present a significant anomaly. DTA reveals that the exothermic reaction P_2 continues while the tests by TEM show that the more the temperature θ_R rises, the more the carbide M_3C tends to evolve to carbide M_7C_3. In addition, a secondary hardening results from the precipitation of very fine carbides M′C and, undoubtedly also, from the type M_2C [10,17–19]. But in this stage, these hardening carbides can not be highlighted.

However, if we compare the curves 2 and 3 of Fig. 9 and that one plots the curve Δ_3^2 representing the difference in hardness

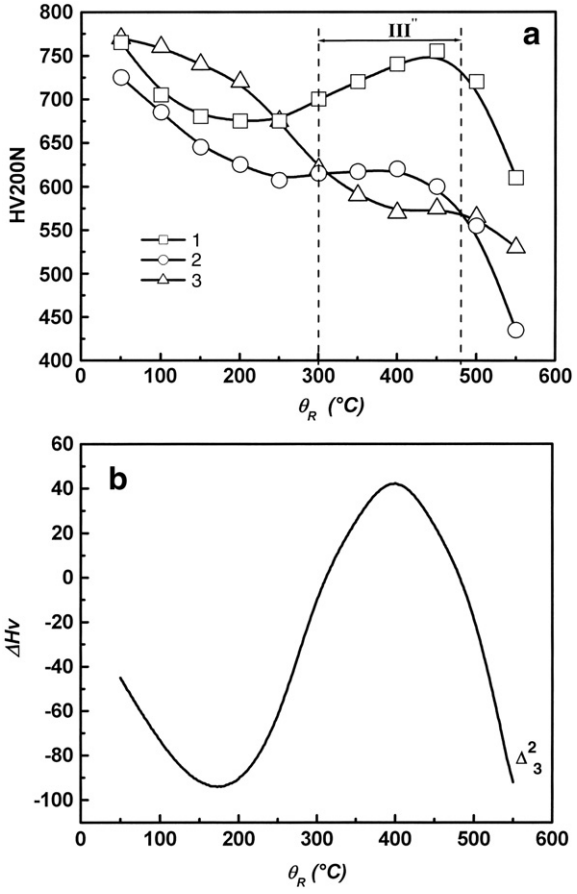

Fig. 9 – Evolution of hardness according to tempering temperature: Curve 1(a), hardness change after treatment of 6 h at θ_R then cooling to 20 °C; Curve 2(a), hot hardness measurement after treatment of 6 h at different temperatures θ_R; Curve 3(a), hot hardness measurement at the beginning of each treatment according to θ_R; Curve Δ_3^2 (b), difference in hardness between curves 2 and 3.

between these two states, we note that there is obviously a gain in hot hardness during an isothermal holdings between 300 and 550 °C approximately. In fact, in this temperature range, there are two successive phenomena:

- The first (towards 300–350 °C) corresponds to the progressive replacement of cementite substituted out of chromium (M_3C precipitated before) by the carbide M_7C_3 with consequent increase in the chromium content.
- The second intervenes mainly between 350 and 550 °C; it is about the precipitation of new substituted carbides, in extremely divided form, within the matrix. These hardening carbides are, according to several authors [10,12,17–19] of the type M_2C — M being mainly of molybdenum — and/or type M′C (V_4C_3). This precipitation takes place within the martensite, which — of this fact — is impoverished clearly in alloy elements. The germination of the carbides M_2C and M′C observed on the level of dislocations, causes (according to Colombier) a distortion of the network of — and a hardening which reaches its maximum whereas these precipitates are hardly discernible even within thin blades observed by electronic microscopy.
- $500<\theta_R<600$ °C (stage III): Hardness tends to decrease with increasing θ_R. Jointly we observe a first expansion in dilatometry, another increase in *J* and an exothermic peak P_3. The precipitates of the types M_7C_3 and M′C grow bigger sufficiently so that they may be observed by TEM; however, this process of enlargement explains the lowering in hardness pointed out here before. It is confirmed that residual austenite can remain stable in this type of steel as for as temperatures much higher than in the case of less charged steels. Till $\theta_R=600$ °C, it remains hot, but it may change in to secondary martensite or bainite only during a cooling down to 20 °C because of its change in composition [20].

The increase in (*J*) is explained rather well owing to the fact that the processes of precipitation continue impoverishing more and more the matrix in alloyed elements. The dilatometric expansion jointly observed is less simple to justify: at the most we can underline a tendency to swelling as the quantity of formed precipitates increases and tend to grow bigger without still coalescing (let us notice that similar phenomena have been observed during the tempering of high speed steels).

Stage IV ($600<\theta_R<650$–700 °C): It is characterized by an another dilatometric expansion, especially visible if the austenitization has been carried out at $\theta_\gamma>1050$ °C. Moreover, the intensity of magnetization *J* decreases slightly then tends to increase again, while the exothermic peak P_3 is split. Hardness continues to decrease gradually (Fig. 9, curve1). These various behaviors correspond to the hot transformation of the residual austenite, destabilized during the preceding stage. In fact, the samples having undergone a tempering at $\theta_R>640$ °C, do not present any more a transformation during the final cooling. Moreover, examination by TEM confirms that the carbides M_7C_3 and M′C are still present and that their mean size is somewhat increased.

Stage V ($700<\theta_R<Ac_1=860$ °C): As long as the Curie point is not crossed($\theta_c=755$–760 °C), the intensity *J* tends to increase; in addition during this stage, the sample contraction which slows down more especially as the temperature θ_R tends towards the Ac_1 temperation. In fact, the preceding observations suggest that the coalescence processes of carbides M_7C_3 and M′C develop from now on significantly.

4. Conclusion

The purpose of this study is to characterize the structural evolutions likely to be developed in a chromium–molybdenum–silicon steel (with a specific addition of vanadium) subjected to tempering after a direct quench from the austenitic field and to estimate their effect on some of the mechanical properties of the material.

Preliminary treatment in the austenitic field led to a limited enrichment of the matrix as long as the temperature is at most equal to 1050 °C; indeed, only carbides of the types M_3C and $M_{23}C_6$ are then dissolved, while carbides of the types M_7C_3 and MC are not very affected. To avoid too significant austenite retention after quenching, this austenizing temperature of 1050 °C was kept: under these conditions, the structural state resulting from a quench at 50 °C/s from 1050 °C consists of a martensitic matrix containing a dispersion of non-dissolved primary carbides M_7C_3 and MC and a volumic fraction of austenite γ_R of about 10 vol.%.

As a first approach of the behavior during the tempering, measurements of hardness were made after isochronous holdings (1 h) at various temperatures: this made it possible to define four successive ranges evolution. These tests were completed by hot hardness measurements, in particular after 6 h of treatment at various temperatures θ_R; the values obtained were compared with those measured after return to 20 °C. It was shown that an isothermal holding in interval 300–450 °C involves a significant increase in hot hardness, associated with the formation of very fine precipitates. Moreover, during final cooling to 20 °C, an additional hardening occurs, resulting from the transformation in secondary martensite or bainite of the austenite γ_R destabilized above 450 °C.

As a second approach, a systematic comparison of the results obtained by various physical methods (dilatometry, differential thermal and thermo-magnetic analysis, observations by TEM) was carried out. The processes developed successively during the tempering show that:

Martensite evolves initially by rejecting carbide ε (at temperature lower than 250 °C), then substituted cementite M_3C (between 250 and 350 °C); this last carbide tends to evolve to the carbide M_7C_3 (between 450 and 500 °C). In parallel intervenes, between 350 and 500 °C, a secondary hardening due to the precipitation in the matrix of carbides of the types Mo_2 C and M′C somewhat substituted. A maximum hardening is observed after tempering at 500 °C (HV300N=725). The process of over-ageing which develop with temperatures θ_R higher than 500 °C, leads to a notable softening.

Residual austenite does not destabilize — by carbide precipitation on the α'/γ interfaces — before 450 °C; it can then transform on cooling, either to bainite, or to secondary martensite. On the other hand, if the heating is continued until higher temperature, this destabilized austenite persists at 600 °C. Between this temperature and 700 °C, this impoverished phase changes finally. At these high temperatures of tempering, there is a formation of carbide of the type M_6C which develop at

the expense of the fine carbides M′C and M_7C_3 formed before which then disappear.

Acknowledgments

This study was carried out thanks to the help of Chavanne-Ketin Company in Berlaimont, which pleasantly provided us the material. We do thank in particular MM. Werquin and Bocquet for profitable discussion.

Many thanks to the director G. Cizeron and technical personnel of the structure of metallic materials laboratory, University of South Paris, Orsay Center, France ,for their sympathy kindness and cooperation.

REFERENCES

[1] Moon HK, Lee KB, Kwon H. Influences of Co addition and austenitizing temperature on secondary hardening and impact fracture behavior in P/M high speed steels of W–Mo–Cr–V(–Co) system. Mater Sci Eng, A 2008;474:328–34.
[2] Durnin J, Ridal KA. Determination of retained austenite in steel by X-ray diffraction. J Iron Steel Inst 1968;206:60–7.
[3] Barralis J, Maeder G. Precis of Metallurgy. Paris: Nathan; 1997.
[4] Fischmeister HF, Ozerskii V, Olsson L. Solidification structure of gas atomized high speed steel powders. Powder Metall 1982;25(1):1–9.
[5] Juřci P, Vojtěch D, Stolař P. Influence of solidification conditions on microstructure and phase composition of a Fe–4C–12Cr–13V alloy. Z Metallkde 1997;88:733–8.
[6] Doubková K, Vojtěch D, Jurči P. Non-equilibrium solidification of high alloy ledeburitic type steel. Metall Mater 1998;36:257–69.
[7] Kusy M, Caplovic L, Grgac P, Vyrostkova A. Solidification microstructures in the rapidly solidified powder of high alloyed V–Cr tool steel. J Mater Process Technol 2004;157–158:729–34.
[8] Bjärbo A, Hättestrand M. Complex carbide growth, dissolution, and coarsening in a modified 12 pet chromium steel—an experimental and theoretical study. M Metall Trans, A 2001;32:19–27.
[9] Výrostková A, Kroupa A, Janice J, Svoboda M. Carbide reactions and phase equilibria in low-alloy Cr–Mo–V steels tempered at 773–993. K Acta Mater 1998;46:31–8.
[10] Pilling J, Ridley N. Tempering of 2.25 Pct Cr–1 Pct Mo Low Carbon Steels. Metall Mater Trans, A 1982;13A:557–63.
[11] Fu RD, Wang TS, Zhou WH, Zhang WH, Zhang FC. Characterization of precipitates in a 2.25Cr–1Mo–0.25V steel for large-scale cast-forged products. Mater Charact 2007;58:968–73.
[12] Godden MJ, Beech J. The M 2 CTOM 6 C Transformation in steels containing molybdenum. J Iron Steel Inst 1970;208:168–73.
[13] Speich GR, Taylor KA. Martensite. In: Olson GB, Owen WS, editors. ASM International; 1992. p. 243–75.
[14] Cheng L, Brakman CM, Korevaar BM, Mittemeijer EJ. The tempering of iron– carbon martensite; dilatometric and calorimetric analysis. Metall Trans, A 1988;19:2415–26.
[15] Sherman AM, Eldis GT, Cohen M. The aging and tempering of iron–nickel–carbon martensites. Metall Trans, A 1983;14:995–1005.
[16] Assefpour-Dezfuly M, Brownrigg A. Parameters affecting sag resistance in spring steels. Metall Trans, A 1989;20:1951–9.
[17] Stiller K, Svensson L-E, Howell PR, Rong W, Andren H-O, Dunlop GL. High resolution microanalytical study of precipitation in a powder metallurgical high speed steel. Acta Metall 1984;32:1457–67.
[18] Karagöz S, Fischmeister HF, Andren H-O, Guang-Jun C. Microstructural changes during overtempering of high-speed steels. Metall Trans, A 1992;23:1631–40.
[19] Rong W, Andren H-O, Wisell H, Dunlop GL. The role of alloy composition in the precipitation behaviour of high speed steels. Acta Metall Mater 1992;40:1727–38.
[20] Dobrzaski LA, Kasprzak W. The influence of 5% cobalt addition on structure and working properties of the 9-2-2-5, 11-2-2-5 and 11-0-2-5 high-speed steels. J Mater Process Technol 2001;109:52–64.